Biochemical and Biophysical Research Communications **290,** 23–28 (2002)
doi:10.1006/bbrc.2001.6185, available online at http://www.idealibrary.com on IDEAL®

Fluorescence Imaging of Metabolic Responses in Single Mitochondria

Satoshi Nakayama, Takanori Sakuyama, Shigeki Mitaku, and Yoshihiro Ohta[1]
Department of Biotechnology, Faculty of Engineering, Tokyo University of Agriculture and Technology, Nakacho, Koganei, Tokyo 184-8588, Japan

Received November 30, 2001

The membrane potentials, rates of NAD(P)H formation, and rates of flavoprotein reduction have been measured for single mitochondria isolated from porcine hearts. These metabolic responses were elicited by the addition of malate and measured using fluorescence microscopy. For the measurements of mitochondrial membrane potential, mitochondria were stained with tetramethylrhodamine ethyl ester, and the membrane potentials of single mitochondria were determined. Individual mitochondria maintained the membrane potential at around −80 mV before addition of malate. Upon the addition of malate, each mitochondrion was rapidly polarized to around −100 ~ −140 mV and underwent repeated cycles of polarization and depolarization, which were probably caused by openings and closings of permeability transition pores. NAD(P)$^+$ and flavoprotein were reduced immediately after addition of malate and then slowly became reoxidized. Thus, single mitochondria can undergo rapid and repetitive changes in membrane potential, but not in the redox state of NAD(P)H and flavoprotein.

Key Words: **mitochondria; fluorescence imaging; metabolic responses; membrane potential; NAD(P)H; flavoprotein; permeability transition; ATP synthesis.**

The transmembrane electrical potential ($\Delta\Psi$m) across the inner mitochondrial membrane has been used as an index of mitochondrial activity. According to the chemiosmotic theory, $\Delta\Psi$m is utilized to provide energy for ATP synthesis. $\Delta\Psi$m is also used by the cell to transport charged molecules and ions into the mitochondrion. The permeability transition (PT) can be examined by measuring $\Delta\Psi$m, because the PT leads to the loss of $\Delta\Psi$m (1). The transient loss of $\Delta\Psi$m induced by the PT allows mitochondria to release Ca^{2+} to the cytosol (2). The PT can also cause release of cytochrome c that leads to apoptosis (3, 4); therefore, a long-lasting decrease in $\Delta\Psi$m is used as an indicator that cells are undergoing apoptosis (5).

Thus far, most of the quantitative studies on $\Delta\Psi$m have been performed using mitochondrial suspensions and have produced the results that help to understand mitochondrial behaviors (6). The $\Delta\Psi$m values measured for these mitochondrial ensembles yield data that have been averaged over a large number of mitochondria. However, measurements of $\Delta\Psi$m in single mitochondria have revealed intracellular heterogeneity of the value (7) as well as the persistence and changes over time of $\Delta\Psi$m (8), although these studies have been qualitative. Also, the fluctuations of $\Delta\Psi$m are not synchronous, even among individual mitochondria (9, 10). These results indicate that quantitative measurements of $\Delta\Psi$m in single mitochondria are necessary to understand patterns of mitochondrial behavior.

Only a small number of studies have reported determinations of $\Delta\Psi$m for single mitochondria (11, 12). These experiments employed a cationic fluorescent dye whose distribution at equilibrium is governed by the Nernst equation to determine $\Delta\Psi$m. The dye concentrations were measured both inside the individual mitochondria and in an adjacent equivalent volume of the cytosol using fluorescence microscopy. To obtain an accurate dye concentration in mitochondria, the out-of-focus fluorescence of the dye was eliminated by deconvolving and restoring fluorescence images using computer algorithms. Although this procedure provides a reasonable method to determine $\Delta\Psi$m even for an intracellular mitochondrion, the results depend theoretically on the size of each mitochondrion (11).

Here we report a procedure to determine $\Delta\Psi$m for a single mitochondrion, independent of its size. This procedure can be used only for isolated mitochondria that do not undergo changes in shape and size during the experiments. The procedure is useful when comparing $\Delta\Psi$m values among different mitochondria, because $\Delta\Psi$m can be obtained independently of mitochondrial

[1] To whom correspondence and reprint requests should be addressed. E-mail: ohta@cc.tuat.ac.jp.

0006-291X/02 $35.00

size. Also, procedures to measure NADH generation and flavoprotein reduction in single mitochondria are described. The methods presented here are helpful for achieving a better understanding of mechanisms such as the PT, that lead to changes in $\Delta\Psi m$, since the behaviors of individual mitochondria are measured directly, rather than averaged over an entire population.

MATERIALS AND METHODS

Preparation of Mitochondria

Porcine heart mitochondria were isolated by differential centrifugation (13) and suspended in isolation medium containing 10 mM Tris–HCl, 250 mM sucrose, 1 mM EDTA, 0.1 mM DTT, pH 7.4. For microscopic measurements, mitochondria were adsorbed onto a glass-bottom culture dish coated with Cell-Tak at around 10^6 mitochondria/dish. They were then kept for 1 h in Tris buffer (10 mM Tris–HCl, 250 mM sucrose, 140 mM KCl, 1 mM EDTA, 0.1 mM DTT) and washed twice with this buffer. All procedures described above were performed at 0–4°C. Each preparation was assayed for ATP production (14) upon addition of 5 mM Na-malate, giving a rate of 363 ± 14 μmol ATP/g/min (mean $\pm$ SE, $n = 6$) which was compatible with the previous results (14, 15). Protein content was determined using the BCA protein assay with BSA as a standard.

Fluorescence Microscopy of Single Mitochondria

The following experiments were performed at 25°C. Prior to the measurements of $\Delta\Psi m$, mitochondria were bathed in buffer A (10 mM Tris–HCl, 250 mM sucrose, 140 mM KCl, 2 mM KH_2PO_4, 0.5 mM ADP, 1 mM EDTA, 0.1 mM DTT) with 1 mg/ml BSA for 30 min. The incubation was carried out in the presence of 2 nM tetramethylrhodamine ethyl ester (TMRE), a dye that is sensitive to changes in potential (8, 10). Before addition of malate or valinomycin, the volume of buffer was 1 ml for all experiments, so that the volume of buffer was $>10^6$ times larger than that of the total mitochondria. When $\Delta\Psi m$ was generated by the diffusion of K^+ in the presence of 20 nM valinomycin, an ionophore for K^+, the extramitochondrial concentration of KCl was decreased to 0.28, 0.47, or 1.4 mM, and NaCl was added in appropriate quantities to compensate for the decrease in osmotic pressure caused by the low KCl concentration. The glass-bottom culture dishes were placed on the stage of an inverted epifluorescence microscope (IX-70, Olympus, Japan) equipped with a 40× objective lens (Uapo40x/340, NA = 0.9, Olympus, Japan). Fluorescence was elicited by illumination with a 75-W xenon lamp through a 15-nm bandpass filter centered at 535 nm. Fluorescence at >580 nm was collected with a cooled CCD camera (PentaMAX 1317K 5 MHz, Princeton Instruments, Trenton, NJ). A series of image frames was acquired at intervals of 3 s, with binning pixels 2×2, under computer control. The exposure time for each frame was 1 s. During the remaining 2 s, the excitation light was cut off with a mechanical shutter to avoid mitochondrial damage that could possibly result from illumination. The intensity of illumination was also reduced to 25% with a neutral density filter to avoid photodynamic injury to mitochondria (8). The readout was digitized to 12 bits, and analyzed with image-processing software (MetaMorph, Universal Imaging Corp., PA).

A fluorescence image of a mitochondrion looks larger than the real mitochondrion due to blurring. For the analysis of individual mitochondria, therefore, the fluorescence intensity was averaged over an area of 9.2 μm^2. This area encompassed even the blurred image of the mitochondrion, and was chosen (i) to reduce the noise by increasing the number of the pixels that were averaged on the fluorescence intensity, (ii) to obtain the fluorescence intensity averaged over the entire mitochondrion. The fluorescence intensity of TMRE in buffer was measured in the same field as mitochondria, but obtained at a position where the fluorescence intensity was not affected by mitochondrial TMRE.

Fluorescence of NAD(P)H within individual mitochondria bathed in buffer A was obtained at wavelengths longer than 420 nm. For the excitation of NAD(P)H, a 20-nm bandpass filter centered at 360 nm was used (16, 17). A neutral density filter was used to attenuate the intensity of illumination to 12%, in order to avoid both photobleaching of NAD(P)H and photodynamic injury to mitochondria. Because the signal to noise ratio of NAD(P)H fluorescence from individual mitochondria was small (S/N of about 1.05 before addition of Na-malate), due to the weak sample fluorescence and the high level of background fluorescence, the exposure time for each image frame was lengthened to 3 s, in an attempt to increase the signal to noise ratio. The time interval between image frames was 5 s. The other procedures for the measurements of NAD(P)H fluorescence were the same as those described for the imaging of TMRE fluorescence. Flavoprotein fluorescence was measured in the same manner as was NAD(P)H fluorescence, except that the flavoprotein was measured at wavelengths of 470-nm excitation and 535-nm emission (16). For each experiment on NAD(P)H and flavoprotein, the image series was background subtracted. A slight photobleaching rate was observed and corrected for by fitting a single exponential plus a constant to the baseline fluorescence signal.

Drugs and Solutions

Twenty nanomolar valinomycin or 3 mM Na-malate was applied by pressure ejection from micropipettes. All solutions were applied to mitochondria with appropriate pH correction. Ethanol, the solvent for rotenone and valinomycin, was used at a maximum concentration of 0.1%, and, when tested alone, did not have significant effects under these experimental conditions. The concentration of TMRE was determined spectrophotometrically with $\epsilon_{549\,nm} = 109\ mM^{-1}\ cm^{-1}$. All experiments with TMRE were performed in buffer A with 1 mg/ml BSA, because nonuniform adsorption of TMRE occurred on a coverslip at the bottom of the dish if BSA was not included. The fluorescence intensity of TMRE must be obtained as the signal proportional to the concentrations of TMRE in mitochondria and in the medium to determine $\Delta\Psi m$. Therefore, nonuniform adsorption interferes with the analysis of $\Delta\Psi m$.

TMRE was obtained from Molecular Probes (Eugene, OR). Rotenone was from Sigma (St. Louis, MO). BCA protein assay reagent was from Pierce Chemical Company (Rockford, IL). Other chemicals were of the highest purity available commercially.

Theoretical Analysis

Kinetics theory of $\Delta\Psi m$ changes upon addition of valinomycin. In the presence of valinomycin, the movements of K^+ and Na^+ across the membrane depend on the differences in the concentrations between the inside and the outside of mitochondria and also depend on the electric potential difference across the membrane. Therefore, when valinomycin is applied to mitochondria at $t = 0$, the changes in the concentrations of K^+ and Na^+ are given by

$$d[K^+]_{in}(t)/dt = k_1 V(t) + k_2\{[K^+]_{in}(t) - [K^+]_{out}(t)\} \quad [1]$$

$$d[Na^+]_{in}(t)/dt = k_3 V(t) + k_4\{[Na^+]_{in}(t) - [Na^+]_{out}(t)\}, \quad [2]$$

where $[K^+]_{in}(t)$ and $[K^+]_{out}(t)$ are concentrations of K^+ at time t inside the mitochondria and in the buffer, respectively, $[Na^+]_{in}(t)$ and $[Na^+]_{out}(t)$ are the concentrations of Na^+ at time t inside the mitochondria and in the buffer, respectively, $V(t)$ is the membrane potential ($\Delta\Psi m$) (inside negative), and k_1, k_2, k_3, and k_4 are constants. Because translocations of K^+ and Na^+ across the membrane lead to

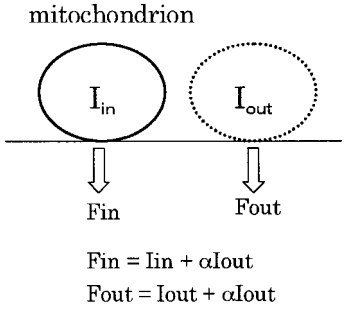

FIG. 1. Schematic illustration of the relationship between apparent and real fluorescence from mitochondria. The circle drawn with a solid line represents a mitochondrion and the circle drawn with a dotted line represents the volume equal to a mitochondrion of the same size. α is a factor that corrects for the fluorescence from the dye that is outside of the mitochondrial volume. $F_{out}(t)$ was obtained at a position where the fluorescence intensity was not affected by mitochondrial TMRE.

polarization or depolarization of the mitochondrial membrane, $V(t)$ is described by using the equation

$$V(t) = V(0) + k_5\{[K^+]_{in}(t) - [K^+]_{in}(0)\} + k_6\{[Na^+]_{in}(t) - [Na^+]_{in}(0)\}, \quad [3]$$

where k_5 and k_6 are constants. Since the volume of buffer is much larger than that of the total mitochondria under the present condition, the concentrations of $[K^+]_{out}(t)$ and $[Na^+]_{out}(t)$ are assumed to be constant and $V(\infty) = 0$. Therefore, $V(t)$ is expressed by the following equation, derived from Eqs. [1], [2], and [3]:

$$V(t) = A * \exp(-B * t) + C * \exp(-D * t) \quad [4]$$

where A, B, C, and D are constants that depend on $[Na^+]_{in}(0)$, $[K^+]_{in}(0)$, $[Na^+]_{out}(0)$, and $[K^+]_{out}(0)$ and the concentration of valinomycin.

Estimation of fluorescence intensity in mitochondria. Since TMRE exists as a monovalent cation in buffer, $V(t)$ is written as follows, according to the Nernst equation at 25°C (18):

$$V(t)\ (mV) = -59 \log(R_1(t)) \quad [5]$$

$$R_1(t) = [TMRE]_{in}(t)/[TMRE]_{out}(t), \quad [6]$$

where $[TMRE]_{in}(t)$ is the concentration of TMRE inside an individual mitochondrion and $[TMRE]_{out}(t)$ is its concentration in the buffer. The apparent fluorescence intensity at the position of a mitochondrion (in the fluorescence images detected with a CCD camera) is a summation of the fluorescence intensities from inside and outside the mitochondrion (see Fig. 1):

$$F_{in}(t) = I_{in}(t) + \alpha I_{out}(t) \quad [7]$$

$$F_{out}(t) = I_{out}(t) + \alpha I_{out}(t), \quad [8]$$

where $I_{in}(t)$ and $I_{out}(t)$ are the fluorescent intensities of TMRE from a mitochondrion and from a volume of buffer that is equal to that of a mitochondrion, respectively. $F_{in}(t)$ and $F_{out}(t)$ are apparent fluorescence intensities of TMRE in the mitochondrion and in the buffer, respectively. α is a constant that represents the effect of fluorescence from outside a mitochondrion, and it depends on the size of the mitochondrion. By applying Eqs. [7] and [8], the following equations are obtained:

$$R_2(t) = (1 + \alpha)\, R_3(t) - \alpha \quad [9]$$

$$R_2(t) = I_{in}(t)/I_{out}(t) \quad [10]$$

$$R_3(t) = F_{in}(t)/F_{out}(t). \quad [11]$$

When the concentration of TMRE is small enough, the fluorescence intensity is proportional to the concentration, i.e., $R_1(t) = R_2(t)$. In these cases, the following equation is derived from Eqs. [4], [5], and [9]:

$$R_3(t) = 1/(1 + \alpha) * \exp[1/59 * \{A * \exp(-B * t) + C * \exp(-D * t)\}] + \alpha/(1 + \alpha) \quad [12]$$

Equation [12] was fitted to the data using a curve-fitting software package (KaleidaGraph, Synergy Software, Reading, PA).

Effects of self-quenching and pH on TMRE fluorescence. The self-quenching of TMRE was analyzed using the following equation according to Vaughan and Weber (19):

$$F([TMRE]) = 0.5 * [TMRE]/\{1 + K * [TMRE]\}, \quad [13]$$

where [TMRE] is the concentration (nM) of TMRE, $F([TMRE])$ is the fluorescence intensity of TMRE at [TMRE] (note that $F([TMRE])$ has been normalized against the fluorescence intensity at 2 nM), and K is a quenching constant. TMRE fluorescence in buffer was measured with a spectrofluorometer (Hitachi F2000). Since (i) $[TMRE]_{out}(t)$ can be assumed to remain at 2 nM during experiments, and (ii) self-quenching of 2 nM TMRE is negligible, $F([TMRE])$ and $0.5 * [TMRE]$ correspond to $R_2(t)$ and $R_1(t)$, respectively. Therefore, $R_1(t)$ is given by

$$R_1(t) = 0.5 * R_2(t)/\{0.5 - K * R_2(t)\}. \quad [14]$$

RESULTS AND DISCUSSION

Voltage-Dependent Accumulation of TMRE in Mitochondria

TMRE was used to monitor the membrane potential changes across the membranes of individual mitochondria. At first, TMRE was examined for (i) voltage-dependent accumulation, and (ii) the absence of nonpotentiometric binding. Voltage-dependent accumulation within the mitochondria was established by polarizing mitochondrial membranes with valinomycin in a medium containing a low concentration of potassium ions (Fig. 2A). The affinity of valinomycin for K^+ is much higher than that for Na^+; therefore, the addition of valinomycin induces fast polarization followed by slow depolarization under these conditions (Fig. 2B). As a control, it was confirmed that application of buffers other than the buffer containing valinomycin induced no significant changes in $R_3(t)$ [in Eq. [11]] over 10 min of recording. This indicated that the movement of ions across the membrane is negligible in the absence of valinomycin under the conditions de-

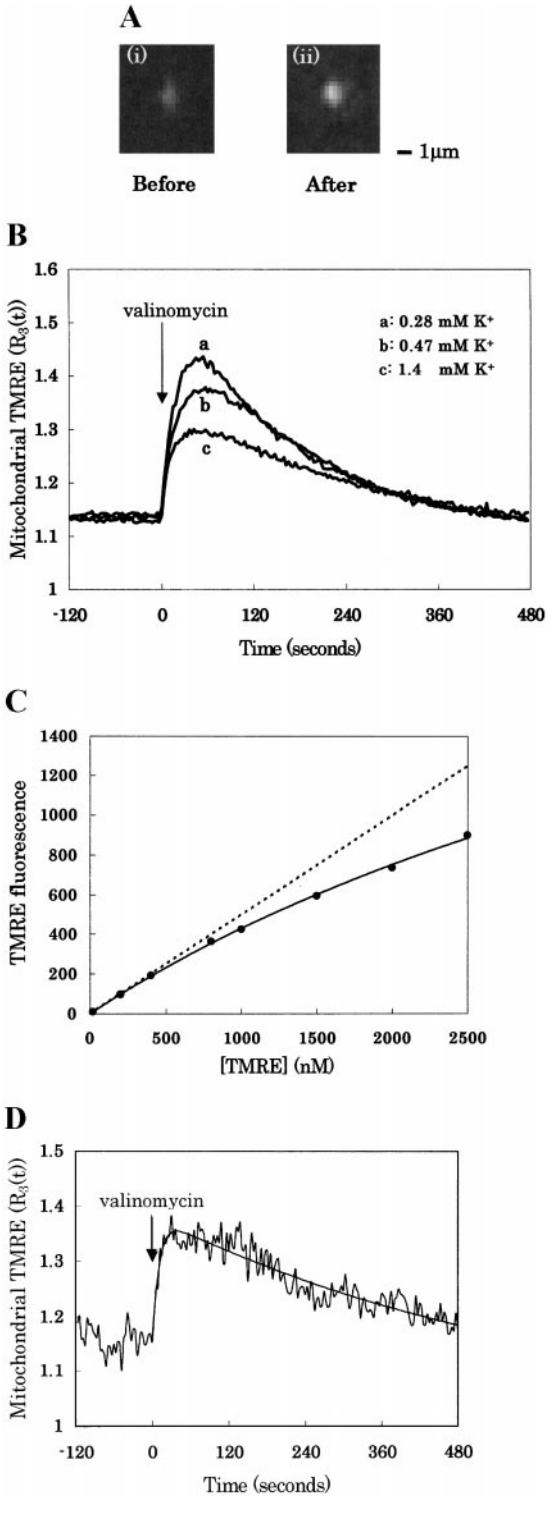

FIG. 2. Voltage-dependent accumulation and self-quenching of TMRE. (A) Fluorescence images of TMRE in mitochondria incubated in the buffer containing 1.4 mM KCl, (i) before addition of valinomycin and (ii) after addition of valinomycin. (B) Voltage-dependent accumulation of TMRE in mitochondria. The vertical axis represents the apparent ratio of TMRE fluorescence in mitochondria to that in buffer, i.e., $R_3(t)$ in Eq. [11]. Potassium concentrations in the buffer are 0.28 mM (curve a), 0.47 mM (curve b), and 1.4 mM (curve c). The decrease in potassium concentration induces a significant increase in $R_3(t)$ after addition of valinomycin. Each curve was obtained by averaging over 30 mitochondria. (C) Analysis of the self-quenching of TMRE. The vertical axis represents the normalized fluorescence intensity of TMRE, $F([\text{TMRE}])$ in Eq. [13]. The solid line was obtained by fitting Eq. [13] to the experimental data (closed circles, ●). A broken line (- - -) shows the theoretical curve in the absence of self-quenching. (D) Time course of valinomycin-induced polarization of a single mitochondrion. The zigzag line represents the data from a single mitochondrion, while the solid curve is obtained by fitting Eq. [12] to the data. At $t = 0$, valinomycin was added to mitochondria that were incubated in buffer containing 1.4 mM K^+.

scribed here. When the potassium concentration in the medium is lowered, addition of valinomycin should induce a large polarization of mitochondria. Therefore, if accumulation of TMRE is driven by electrical potential differences, the maximum value of $R_3(t)$ should be larger in individual mitochondria that have a lower concentration of potassium in the medium. Results of experiments testing this idea are shown in Fig. 2B, and they indicate that TMRE is indeed accumulated within the mitochondria in a voltage-dependent manner.

The absence of nonpotentiometric binding was confirmed by depolarizing mitochondria with the potassium-selective ionophore valinomycin. When mitochondria were incubated in a high (140 mM) KCl medium, the addition of valinomycin completely abolished the contrast between the mitochondria and the buffer (data not shown). This indicates that passive binding of the dye to mitochondria was so low that it could not be detected.

Effects of Self-Quenching and pH on the Fluorescence Intensity of TMRE

Fluorescent molecules exhibit self-quenching at high concentrations. Therefore, self-quenching of TMRE could occur in mitochondria having a large $\Delta\Psi m$. To estimate the effects of self-quenching on the fluorescence intensity, the fluorescence intensity of TMRE was measured as a function of its concentration and analyzed using Eq. [13]. The results are shown in Fig. 2C. TMRE showed self-quenching as its concentration increased. The quenching constant was 0.000165 (nM^{-1}). The influence on the TMRE fluorescence of pH changes, which could occur during mitochondrial respiration, was excluded by testing a series of solutions of TMRE in the spectrofluorometer. pH variations in the range from 6.9 to 10.5 failed to produce significant effects on the fluorescence intensity of TMRE (data not shown).

Estimation of the Effect of Extramitochondrial TMRE on Apparent Mitochondrial Fluorescence

To estimate the effect of α on the apparent mitochondrial fluorescence $R_3(t)$, valinomycin was added to mitochondria that were incubated in medium containing

1.4 mM K^+. If it is assumed that the concentration of K^+ in the matrix space is 140 mM, the maximum concentration of TMRE in mitochondria is calculated to be less than 200 nM (by the Nernst equation). Since self-quenching of TMRE at 200 nM is negligible (around 3% of the total fluorescence, see Fig. 2C), it was possible to determine the value of α. By fitting Eq. [12] to the data (Fig. 2D), the parameters of Eq. [12] were obtained. Calculated values were $\alpha = 283$, A = −58.14, B = 0.075, C = 262.2, and D = 0.0005, all averaged over 50 mitochondria. It should be noted that $R_3(t)$ was not affected by the increase in volume of the buffer upon addition of valinomycin in these experiments.

Determination of Malate-Induced ΔΨm in Single Mitochondria

Changes in TMRE fluorescence were measured after addition of malate to the mitochondria. In most energized mitochondria, rapid but transient depolarizations of the membrane were observed (Fig. 3A). The repetitive polarizations and depolarizations did not cease during recording. Oscillations of ΔΨm can be caused by the openings and the closings of the permeability transition pore (PTP) (9, 10). The polarization by the addition of valinomycin did not induce oscillations of ΔΨm (Fig. 2D), suggesting that the openings and closings of PTP could be metabolic responses of mitochondria.

To determine the absolute value of the malate-induced ΔΨm in single mitochondria, 1 μM rotenone was added after recording malate-induced changes in ΔΨm. Rotenone stops changes in ΔΨm by inhibiting the supply of electrons to the electron transport chain. After confirming that ΔΨm became stable, the K^+ concentration was decreased to 1.4 mM. Next, valinomycin was added to determine α for each mitochondrion. After obtaining an α value for each mitochondrion, $R_2(t)$, $R_1(t)$, and $V(t)$ were calculated according to Eqs. [9], [14], and [5], respectively. Before the addition of malate, mitochondria maintained their membrane potentials at around −80 mV. Upon addition of malate, the membrane potentials changed to around −140 mV and then fluctuated mostly in the range between −100 and −140 mV (Fig. 3B). These values are consistent with previous reports for coupled mitochondria (20). Because α values reflect the size of mitochondria, we examined the correlation between size and ΔΨm. No significant correlation was found (Fig. 3C).

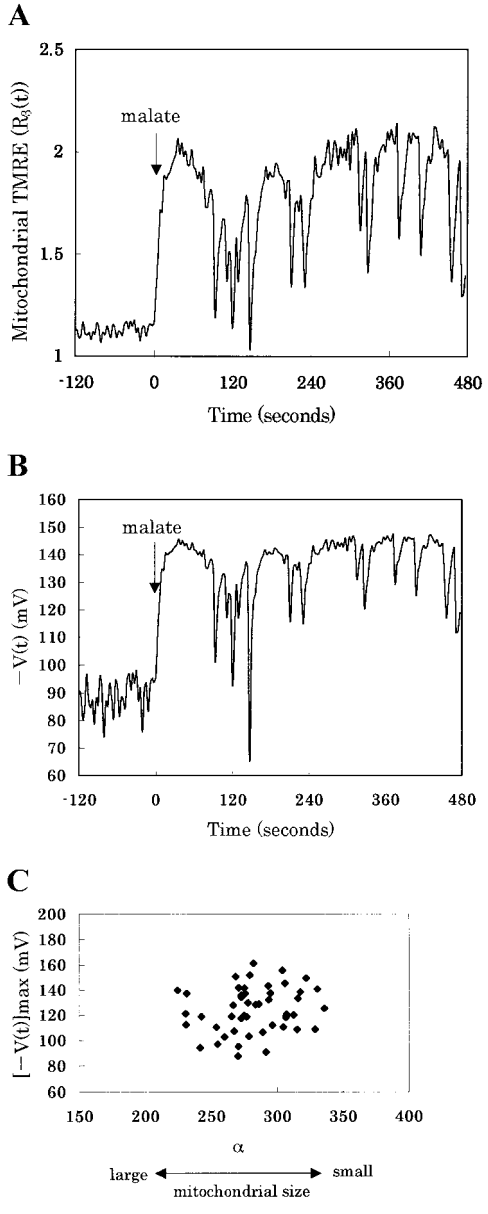

FIG. 3. Membrane potentials induced by the addition of malate were observed for single mitochondria. (A) The vertical axis represents apparent TMRE fluorescence of a single mitochondrion, $R_3(t)$. (B) After the determination of α for the same mitochondrion as that in (a), the vertical axis was converted to millivolts by solving Eqs. [5], [9], and [14]. (C) Distributions of α versus the maximal values of ΔΨm generated by malate. Each dot corresponds to a measurement made on a different single mitochondrion.

NAD(P)H Formation and Flavin Reduction in Single Mitochondria

In addition to ΔΨm generation, mitochondrial responses include NAD(P)H formation and flavoprotein reduction (16, 21). These metabolic responses were recorded in single mitochondria. Upon addition of malate, a rapid increase in NAD(P)H fluorescence was observed, followed by a gradual decrease (Fig. 4A), indicating rapid generation and a gradual subsequent decay of NAD(P)H. In contrast to changes in ΔΨm, the time course of NAD(P)H concentration in single mitochondria did not show appreciable variation among the individual mitochondria. Flavoprotein was reduced rapidly by the addition of malate and was then reoxi-

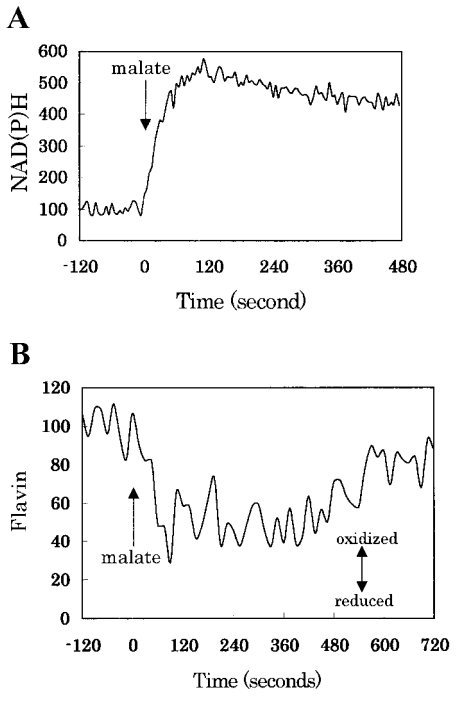

FIG. 4. Time-resolved NAD(P)H and flavin fluorescence in single mitochondria. The addition of malate induced (A) the generation of NAD(P)H and (B) the reduction of flavoproteins. For both curves, average values before addition of malate were normalized to 100.

dized slowly (Fig. 4B). These results indicate that the consumption of NAD(P)H and the oxidation of flavoprotein are gradual processes, even though $\Delta\Psi m$ dissipates rapidly and then is regenerated quickly during ATP synthesis.

ACKNOWLEDGMENTS

We thank Koichi Watanabe, Emiko Ohwashi, and Tomohiro Hattori for their technical assistance. This work was funded by grants from the Ministry of Education, Science, and Culture in Japan and the Nissan Science Foundation.

REFERENCES

1. Fontaine, E., Erikson, O., Ichas, F., and Bernardi, P. (1998) Regulation of the permeability transition pore in skeletal muscle mitochondria. *J. Biol. Chem.* **273,** 12662–12668.
2. Ichas, F., Jouaville, L. S., and Mazat, J.-P. (1997) Mitochondria are excitable organelles capable of generating and conveying electrical and calcium signal. *Cell* **27,** 1145–1153.
3. Bradham, C. A., Qian, T., Streetz, K., Trautwein, C., Brenner, D. A., and Lemasters, J. J. (1998) The mitochondrial permeability transition is required for tumor necrosis factor-alpha mediated apoptosis and cytochrome *c* release. *Mol. Cell. Biol.* **18,** 6353–6364.
4. Inoki, Y., Miura, T., Kajimoto, T., Kawase, M., Kawase, Y., Yoshida, Y., Tsuji, S., Kinouchi, T., Endo, H., Kagawa, Y., and Hamamoto, T. (2000) Ganglioside GD3 and its mimetics induce cytochrome *c* release from mitochondria. *Biochem. Biophys. Res. Commun.* **276,** 1210–1216.
5. Ichas, F., and Mazat, J.-P. (1998) From calcium signaling to cell death: Two conformations for the mitochondrial permeability transition pore. Switching from low- to high-conductance state. *Biochim. Biophys. Acta* **1366,** 33–50.
6. Narita, M., Shimizu, S., Ito, T., Chittenden, T., Lutz, R. J., Matsuda, H., and Tsujimoto, Y. (1998) Bax interacts with the permeability transition pore to induce permeability transition and cytochrome *c* release in isolated mitochondria. *Proc. Natl. Acad. Sci. USA* **95,** 14681–14686.
7. Smiley, S. T., Reers, M., Mottola-Hartshorn, C., Lin, M., Chen, A., Smith, T. W., Steele, G. D., Jr., and Chen, L. B. (1991) Intracellular heterogeneity in mitochondrial membrane potentials revealed by a J-aggregate-forming lipophilic cation JC-1. *Proc. Natl. Acad. Sci. USA* **88,** 3671–3675.
8. Duchen, M. R., Leyssens, A., and Crompton, M. (1998) Transient mitochondrial depolarizations reflect focal sarcoplasmic reticular calcium release in single rat cardiomyocytes. *J. Cell Biol.* **142,** 975–988.
9. Hüser, J., Rechenmacher, C. E., and Blatter, L. A. (1998) Imaging the permeability transition in single mitochondria. *Biophys. J.* **74,** 2129–2137.
10. Hüser, J., and Blatter, L. A. (1999) Fluctuation in mitochondrial membrane potential caused by repetitive gating of the permeability transition pore. *Biochem. J.* **343,** 311–317.
11. Loew, L. M., Tuft, R. A., Carrington, W., and Fay, F. S. (1993) Imaging in five dimensions: Time-dependent membrane potentials in individual mitochondria. *Biophys. J.* **65,** 2396–2407.
12. Fink, C., Morgan, F., and Loew, L. M. (1998) Intracellular fluorescent probe concentrations by confocal microscopy. *Biophys. J.* **75,** 1648–1658.
13. Palmer, J. W., Tander, B., and Hoppel, C. L. (1977) Biochemical properties of subsarcolemmal and interfibrillar mitochondria isolated from rat cardiac muscle. *J. Biol. Chem.* **252,** 8731–8739.
14. Wibom, R., Lundin, A., and Hultman, E. (1990) A sensitive method for measuring ATP-formation in rat muscle mitochondria. *Scand. J. Clin. Lab. Invest.* **50,** 143–152.
15. Wibom, R., and Hultman, E. (1990) ATP production rate in mitochondria isolated from microsamples of human muscle. *Am. J. Physiol.* **259,** E204–E209.
16. Hajnóczky, G., Robb-Gaspers, L. D., Seitz, M. B., and Thomas, A. P. (1995) Decoding of cytosolic calcium oscillations in the mitochondria. *Cell* **82,** 415–424.
17. Robb-Gaspers, L. D., Burnett, P., Rutter, G. A., Denton, R. M., Rizzuto, R., and Thomas, A. P. (1998) Integrating cytosolic calcium signals into mitochondrial metabolic responses. *EMBO J.* **17,** 4987–5000.
18. Brand, M. (1995) Measurements of mitochondrial proton motive force. *In* Bioenergetics (Brown, G. C., and Cooper, C. E., Eds.), pp. 39–62, Oxford Univ. Press, Oxford, NY.
19. Vaughan, W. M., and Weber, G. (1970) Oxygen quenching of pyrenebutyric acid fluorescence in water. A dynamic probe of the microenvironment. *Biochemistry* **9,** 464–473.
20. Degli Esposti, M. (2001) Assessing functional integrity of mitochondria *in vitro* and *in vivo. Methods Cell Biol.* **65,** 75–96.
21. Scholz, R., Thurman, R. G., Williamson, J. R., Chance, B., and Bücher, T. (1969) Flavin and pyridine nucleotide oxidation–reduction changes in perfused rat liver. *J. Biol. Chem.* **244,** 2317–2324.